

Electronic Supplementary Information: Tailoring Dielectric Properties using Designed Polymer- Grafted ZnO Nanoparticles in Silicone Rubber

Martin Wählander^a, Fritjof Nilsson^a, Richard L. Andersson^a, Carmen Cobo Sanchez^a, Nathaniel Taylor^b, Anna Carlmark^a, Henrik Hillborg^{a,c}, Eva Malmström^{a,*}

^aSchool of Chemical Science and Engineering, Department of Fibre and Polymer Technology and ^bSchool of Electrical Engineering, Department of Electromagnetic Engineering, KTH Royal Institute of Technology, SE-100 44 Stockholm, Sweden, *Corresponding author: mavam@kth.se

^cABB AB, Corporate Research, Power Technology, SE-721 78 Västerås, Sweden

Comparison of commercial ZnO NPs

Depending on the manufacturing method, the NPs may contain various amounts of impurities. We compared two commercial NPs produced from salt (ZnO-precip) with NPs produced by flame spray pyrolysis (ZnO-plasma). The two types of ZnO gave rise to different FTIR spectra. The ZnO-precip contained residues such as ZnCO₃ of the precursor Zn₅(CO₃)₂(OH)₆,² which was detected at 1394 cm⁻¹ and 1506 cm⁻¹. These peaks were absent in ZnO-plasma (Fig.S1). The broad absorption peaks of hydroxyl groups (2900-3600 cm⁻¹) were present in both samples. The ZnO-plasma was ten times more pure (ten times less organic content) than the ZnO-precip, according to TGA (Fig.S2). The resistivity of nanocomposites (Sylgard[®] 184) filled with 15 vol.% (~84 wt%) of either ZnO-precip or ZnO-plasma was determined (Fig.S3). The resistivity increased by 2-4 orders of magnitudes at room temperature with electrical fields ranging from 0.1 kV mm⁻¹ to 6 kV mm⁻¹ when pure ZnO-plasma was used as nanofiller rather than ZnO-precip. This study confirms the importance of using NPs which are as pure and well-defined as possible.

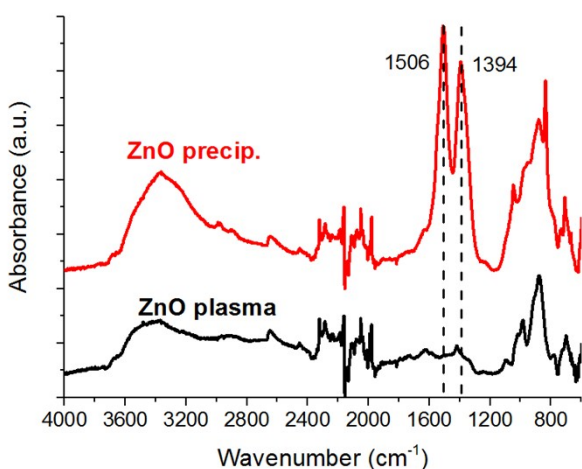


Fig.S1 Normalized FTIR spectra of “ZnO-plasma” and “ZnO-precip” NPs. Broad absorption peaks at 2900–3600 cm⁻¹ can be observed in both samples due to stretching vibration of the hydrogen bond. In the “ZnO-precip” sample, the peaks at 1394 cm⁻¹ and 1506 cm⁻¹ indicate the presence of remnants of ZnCO₃ from the precursor Zn₅(CO₃)₂(OH)₆.²

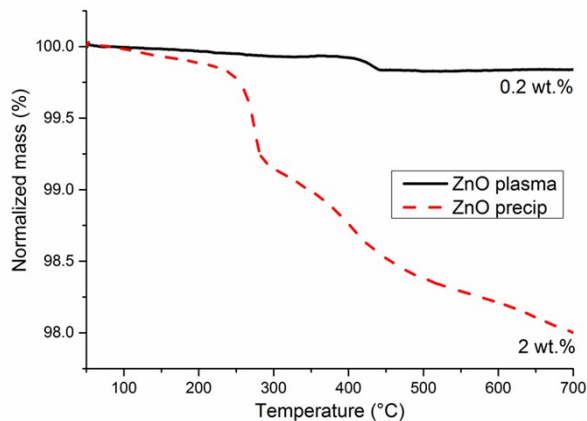


Fig.S2 Comparative thermograms of commercial ZnO, produced by (black curve) flame spray pyrolysis (plasma) or (red curve) precipitation of zinc salt precursors. The amount of volatile organic compounds is about 10 times higher (2 wt.%) in “ZnO precip” than in “ZnO-plasma” (0.2 wt.%).

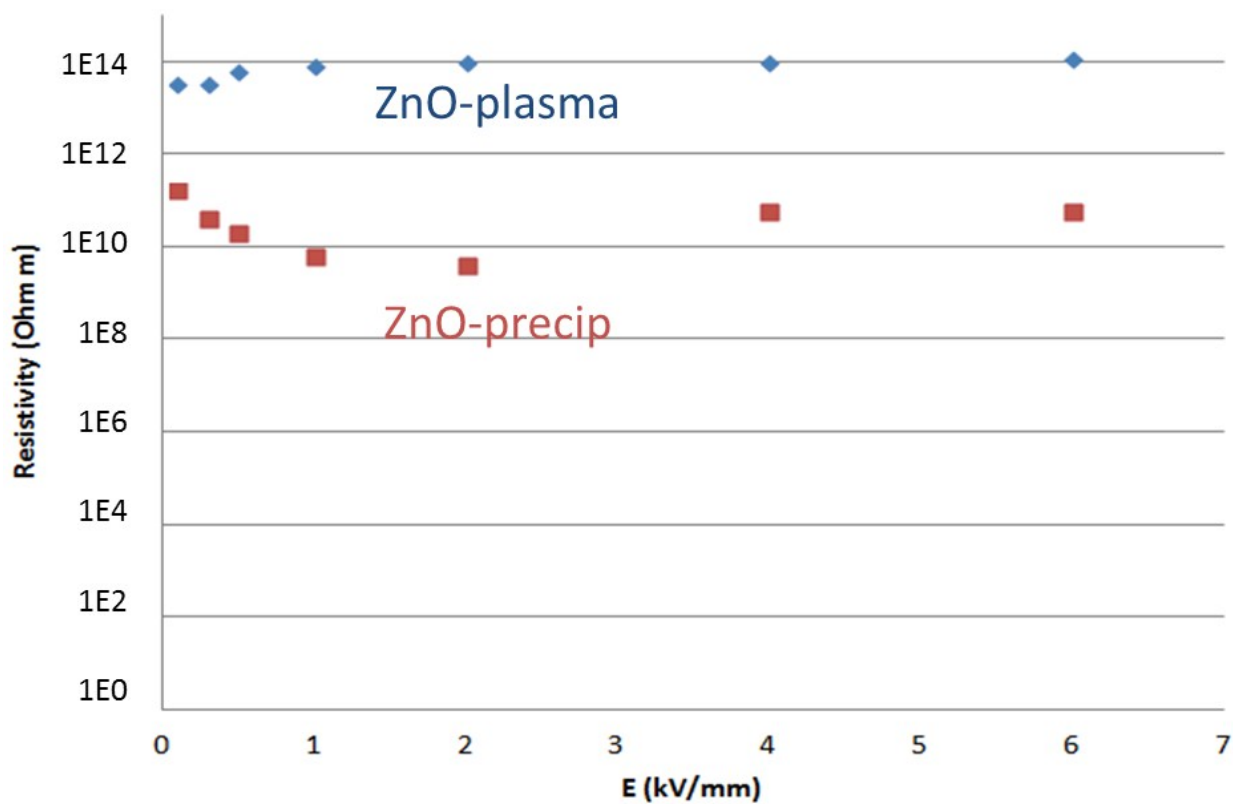


Fig.S3 The resistivity plotted against the electrical field ranging from 0.1 kV mm^{-1} to 6 kV mm^{-1} at RT of nanocomposites with 15 vol.% of ZnO NPs produced by either flame-spray pyrolysis (blue diamonds, “ZnO-plasma”) or salt-precipitation (red squares, “ZnO-precip”).

Experimental

Silanization of ZnO-NPs (ZnO-APTES)

In a general silanization procedure, the ZnO NPs (8.0 g) were dried in vacuum (<1 mbar) at 190 °C were added to 400 mL EtOH:H₂O solution (1:1 by vol.). The suspension was first stirred by a magnet for 3 h, thereafter dispersed in an ultrasonication bath (5 min) and finally by ultrasonic microtip (diameter of 13 mm, four times 1.5 min @ 27 % ampl.). APTES (12 mL, 160 mmol) was added drop-wise to the homogeneous suspension during intense magnetic stirring and refluxed in EtOH for 3 h. The product of silanized ZnO (ZnO-APTES) was purified by three cycles of centrifugation (20 000 xg, 15 min, 18 °C) and homogenization in an ultrasonication bath (5 min) while shaking and by ultrasonic microtip (diameter 5 mm, twice for 1 min, 27 % ampl.). The first cycle was performed in EtOH:H₂O solution (1:1 by vol.) and the second in pure EtOH. The purified ZnO-APTES was stored in EtOH. A small amount of NPs (150 mg) was dried under vacuum at 50 °C overnight and analyzed by Kaiser-test FTIR, TGA, SEM and TEM.

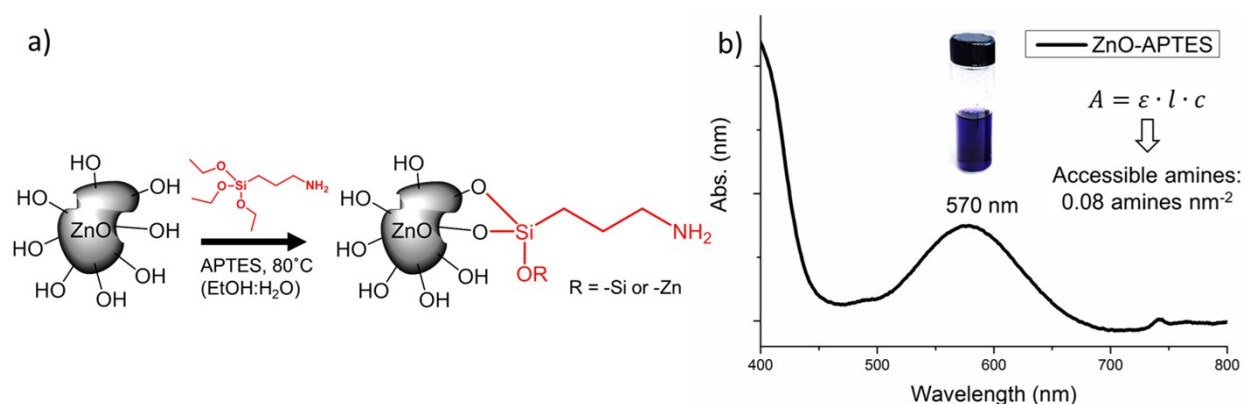


Fig.S4 a) A schematic silanization reaction of ZnO NP with APTES (red) to form ZnO-APTES. b) Light absorption by the blue ninhydrin-complex at 570 nm obtained from the accessible primary amines in ZnO-APTES using the Kaiser-test.

Immobilization of initiator to ZnO NPs (ZnO-Br)

The immobilization was generally performed in batches of 3.7 g of ZnO-APTES. The EtOH was exchanged to EtOH:THF (1:1 by vol.) and finally to pure THF during three cycles of centrifugation/dispersion. The centrifugation was performed at 20 000 xg for 15 min at 15 °C and the dispersion by ultrasonic microtip (diameter 5mm, twice for 1 min @ 27 % ampl.). In general, ZnO-APTES was dispersed in pure THF (230 mL) in an Erlenmeyer flask and DMAP (catalytic amount), TEA (444 μ L, 3.18 mmol) and α -BiB (338 μ L, 2.74 mmol) were added. The flask was sealed and the mixture was allowed to react for 20 h on a shaking device. The reaction was quenched by the addition of EtOH and the initiator-immobilized ZnO (ZnO-Br) were purified by four cycles of centrifugation/ultrasonication while the polarity of the solvent was exchanged starting from THF:EtOH (1:1 by vol.), through pure THF, followed by toluene:THF (1:1 by vol.) and finally pure toluene. ZnO-Br was stored in toluene until further use. A small amount (150 mg) of ZnO-Br was dried under vacuum at 50 °C overnight. The dried ZnO-Br was analyzed by FTIR and TGA. From the mass loss of TGA, the average amount of Br-groups was calculated to be 0.021 μ mol Br mg⁻¹ ZnO-Br.

Purification of ZnO-g-PBMA

The solvents used in the first cycle were toluene:THF (1:1 by vol.), followed by THF:H₂O (1:1 by vol.) and finally three cycles of pure THF. The centrifugation was performed at 30000xg for 10-20 min at 15 °C using 50 mL PPCO centrifuge tubes (Oak Ridge) with a round bottom. The supernatant containing the free PBMA was exchanged by pure solvent and the sediment of grafted NPs was redispersed by ultrasonication in a bath, shaking and by ultrasonication using a Sonic Vibra cell, Autotune Series High Intensity Ultrasonic Processor, equipped with a microtip (diameter 5 mm, twice for 1 min @ 27 % ampl.) directly into the centrifugation tubes cooled by an ice-bath.

Cleaving of PBMA grafts, a general procedure

TBAF (ca 1 ml, 1 M in THF) was added to ZnO-g-PBMA (100 mg of in 10 ml THF) (Fig.S4) After ultrasonication for 20 min in an ultrasonication bath, the samples were left for a week at ambient temperature on a shaking device. Thereafter, the degrafted ZnO was separated from the orange-pink supernatant by centrifugation (20 000xg, 10 min, 20 °C). The THF was removed by rotevaporation and the TBAF was precipitated by the addition of diethyl ether, followed by filtration. Finally, the grafts concentrated by rotevaporation and dried under vacuum at 50 °C. The cleaved PBMA-grafts were analyzed by DMF-SEC. The degrafted ZnO were characterized by FIIR to confirm the successful cleaving of the grafts.

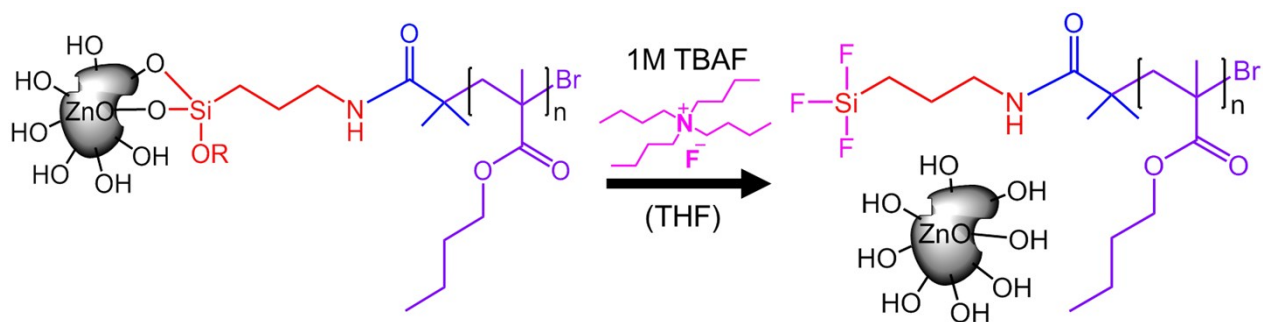


Fig.S5 Cleaving of grafts from ZnO-g-PBMA using TBAF.

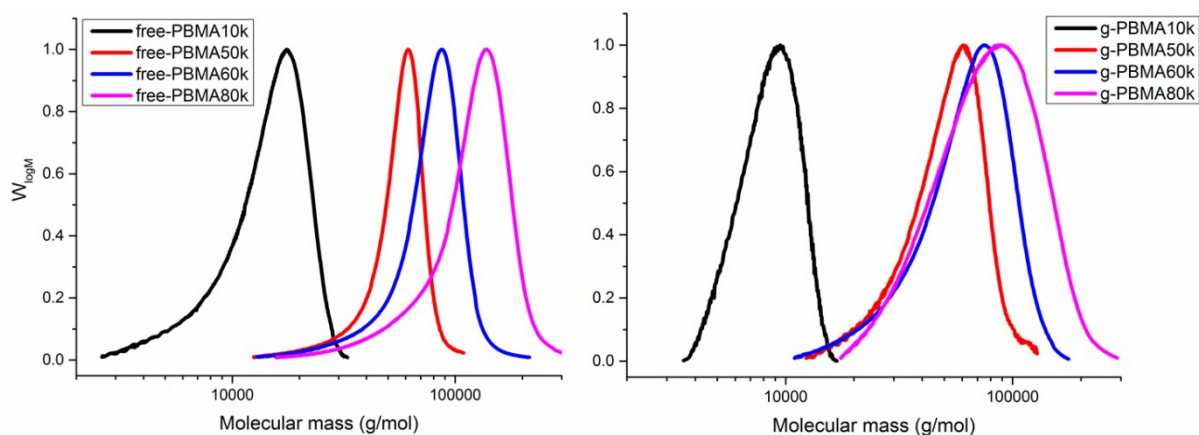


Fig.S6 Free PBMA-chains and cleaved PBMA-grafts characterized by DMF-SEC.

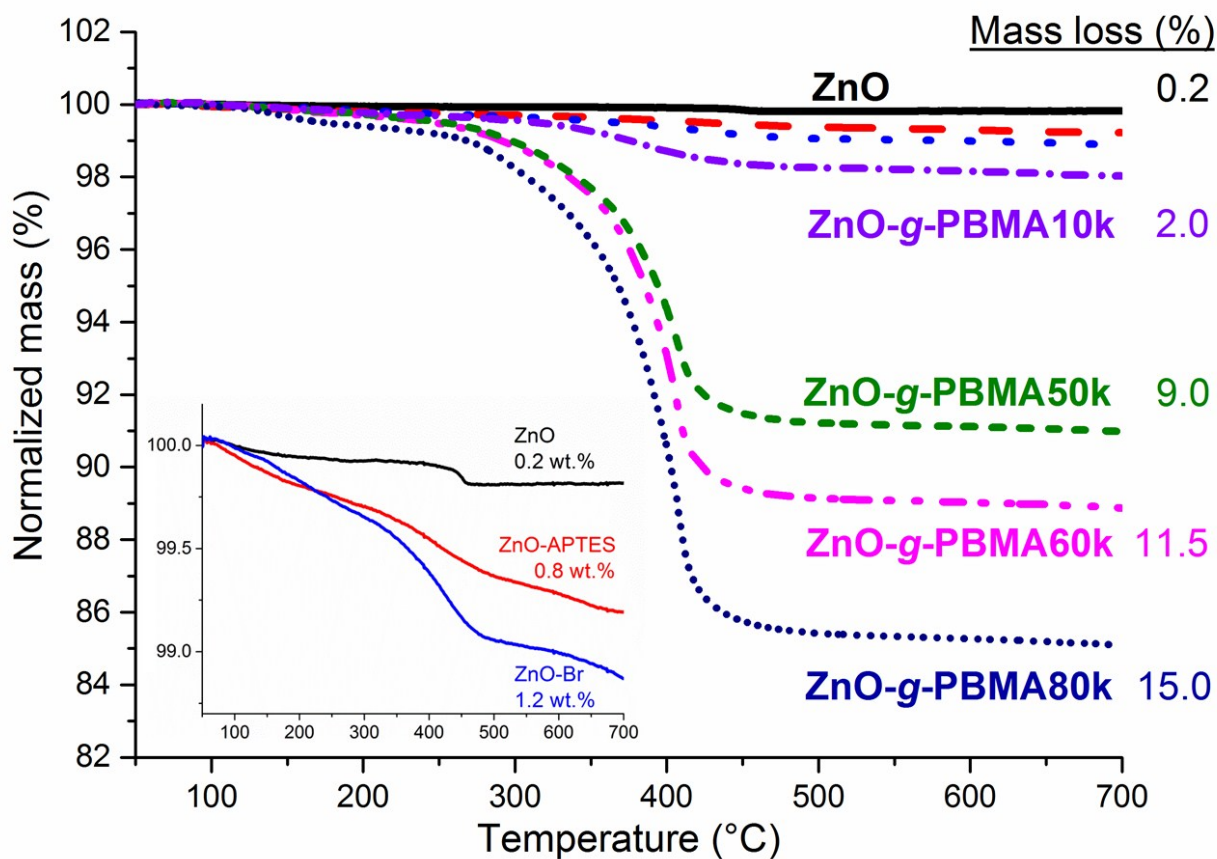


Fig.S7 Thermograms showing the mass loss of ZnO, ZnO-APTES, ZnO-Br and ZnO-g-PBMA with 10 kDa, 50 kDa, 60 kDa and 80 kDa of graft length between 50 °C and 700 °C in N₂. The insert shows detailed thermograms and the mass loss of ZnO, ZnO-APTES and ZnO-Br.

Hansen's solubility parameters (HSP)

Table S1. Hansen's solubility parameters of silicone, ZnO, PBMA and THF.

	δ_D	δ_P	δ_H	R_0
Silicone resin (Baysilone)	19.4	9.9	10.1	6.9
ZnO #1	16.9	7.8	10.6	13.2
ZnO #2	16.2	10.8	12.7	9.8
PBMA	15.9	5.5	5.9	8.5
THF	16.8	5.7	8	-

Using the HSP values in Table S1 and eq.1 and RED, the compatibility of ZnO in silicone was found to be good (RED = 0.41-0.71), allowing homogeneous nanocomposites to be fabricated.

Both PBMA and THF were found to be semi-compatible in silicone as the REDs were equal to 1.09 and 1.01, respectively. PBMA-grafted NPs suspended in THF would theoretically give heterogeneous structures in silicone.

The solubility of PBMA in THF was found to be good (RED = 0.33). Therefore, the ZnO NPs with PBMA-grafts were well suspended in THF.

Calculation of M_g from organic content and grafting density

The accessible amine concentration (σ_{amine}) detected by the Kaiser-test was 0.08 amines nm^{-2} , which corresponds well to the final grafting density (σ_{graft}). The theoretical molecular weight of the PBMA-grafts was calculated based on the σ_{amine} and the organic mass loss in TGA, according to:

$$M_g = \frac{X_g \cdot N}{(1 - X_g) \cdot \sigma_{amine} \cdot 10^{18} \cdot SSA} \quad (\text{eq. S1})$$

where X_g is the mass fraction of grafts, N is Avogadro's number and SSA is the specific surface area of dry ZnO NPs.

Band-gap of pristine and grafted ZnO NPs

The absorption spectrum of ZnO depends on the morphology and size of the particles. Larger ZnO NPs or aggregates red-shift the absorption peak to longer wavelengths. A narrow NP dispersion gives a steeper slope and a more narrow absorption peak.

The energy difference between the valence band and the conducting band is called the band gap. Undoped macroscopic ZnO is a semiconductor with a large band gap ($E_g^{\text{bulk}} \approx 3.3$ eV). The band gap of ZnO NPs in dispersion was determined by the wavelength of the absorption peak according to Planck's equation³:

$$E_g = h\nu = \frac{hc}{\lambda} \approx \frac{1240}{\lambda} \quad (\text{eq. S2})$$

where h is Planck's constant (4.14×10^{-15} eVs), c is the speed of light (2.99×10^8 m/s) and λ is the wavelength of the maximum absorbance.

The UV absorption pattern of ZnO was preserved after grafting. However, a slight shift of the absorbance peak from 375.5 nm to 372.5 nm was observed upon grafting, which caused a slight increase in the band gap (Fig.S8, Table S2). As a result of the improved dispersion of ZnO-g-PBMA, a pronounced absorbance slope and pronounced peak-region < 375 nm was observed.

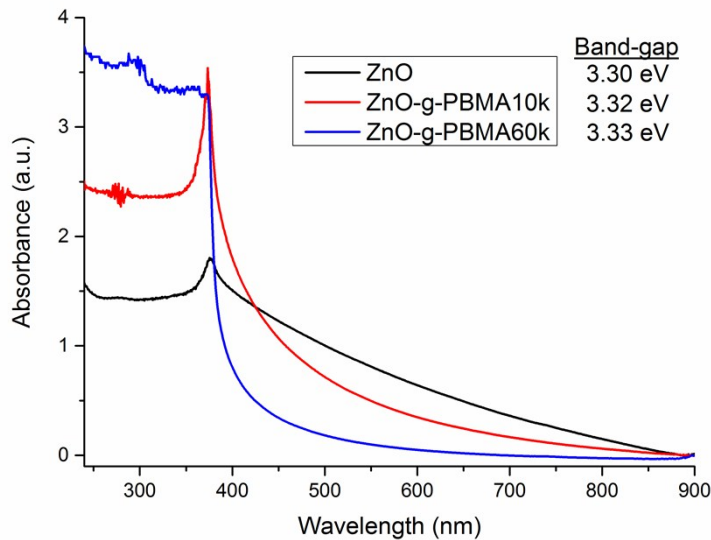


Fig.S8. The absorbance of ZnO, ZnO-g-PBMA10k and ZnO-g-PBMA60k. A sharp peak at 375 nm indicates a narrow particle distribution. Note that the slope of the absorbance increases for dispersed samples of similar size. The absorbance between 450-375 nm was dramatically greater for ZnO-g-PBMA60k. The absorbance correspond to a band gap of ~3.3 eV.

Table S2. The wavelength at peak abs. and the band-gap energy from UV-Vis absorption spectra (Fig.S8).

Sample	Wavelength @ peak absorbance, λ (nm)	Band-gap, E_g (eV)
ZnO	375.5	3.30
ZnO-g-PBMA10k	373.5	3.32
ZnO-g-PBMA60k	372.5	3.33

Silicone nanocomposites

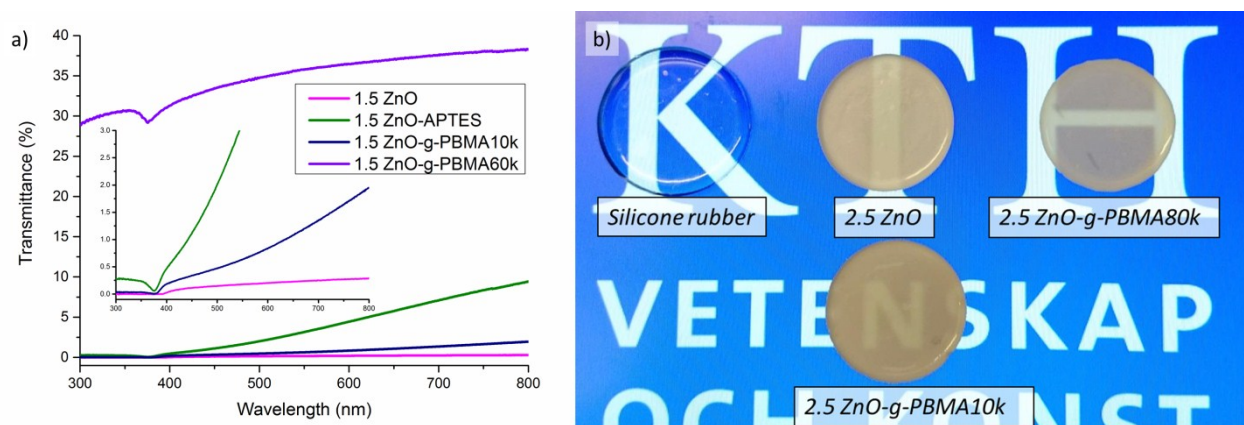


Fig.S9 a) Transmittance of nanocomposites with 1.5 vol.% ZnO NPs. b) Photographs of neat silicone rubber and nanocomposites with 2.5 vol.% ZnO NPs (thickness: ~ 0.4 mm)

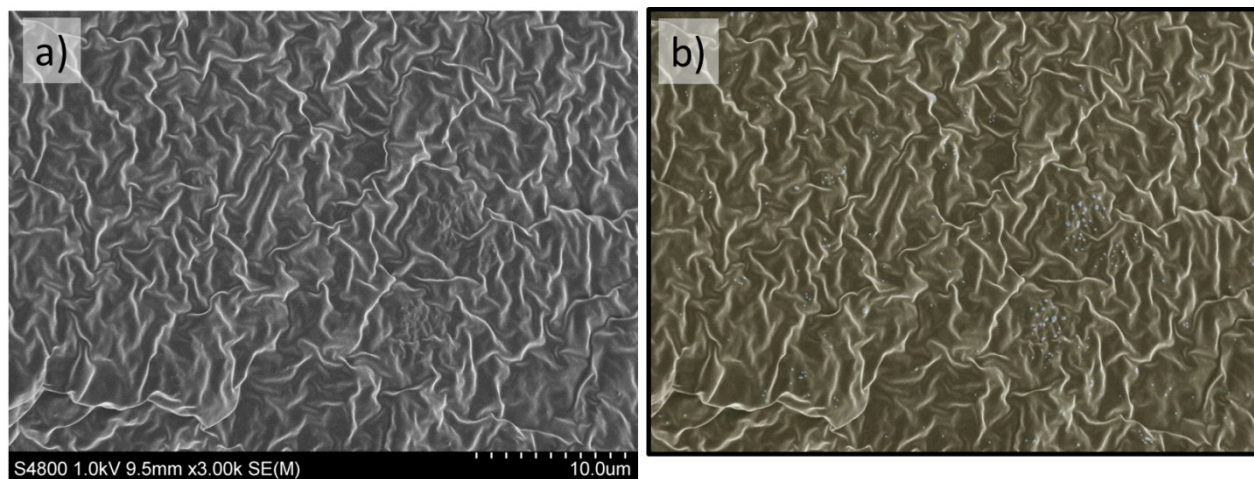


Fig.S10 a) Original SEM image and b) colorized SEM image of the cross-section highlighting the randomly distributed pristine ZnO in 1.5 ZnO (light blue NPs).

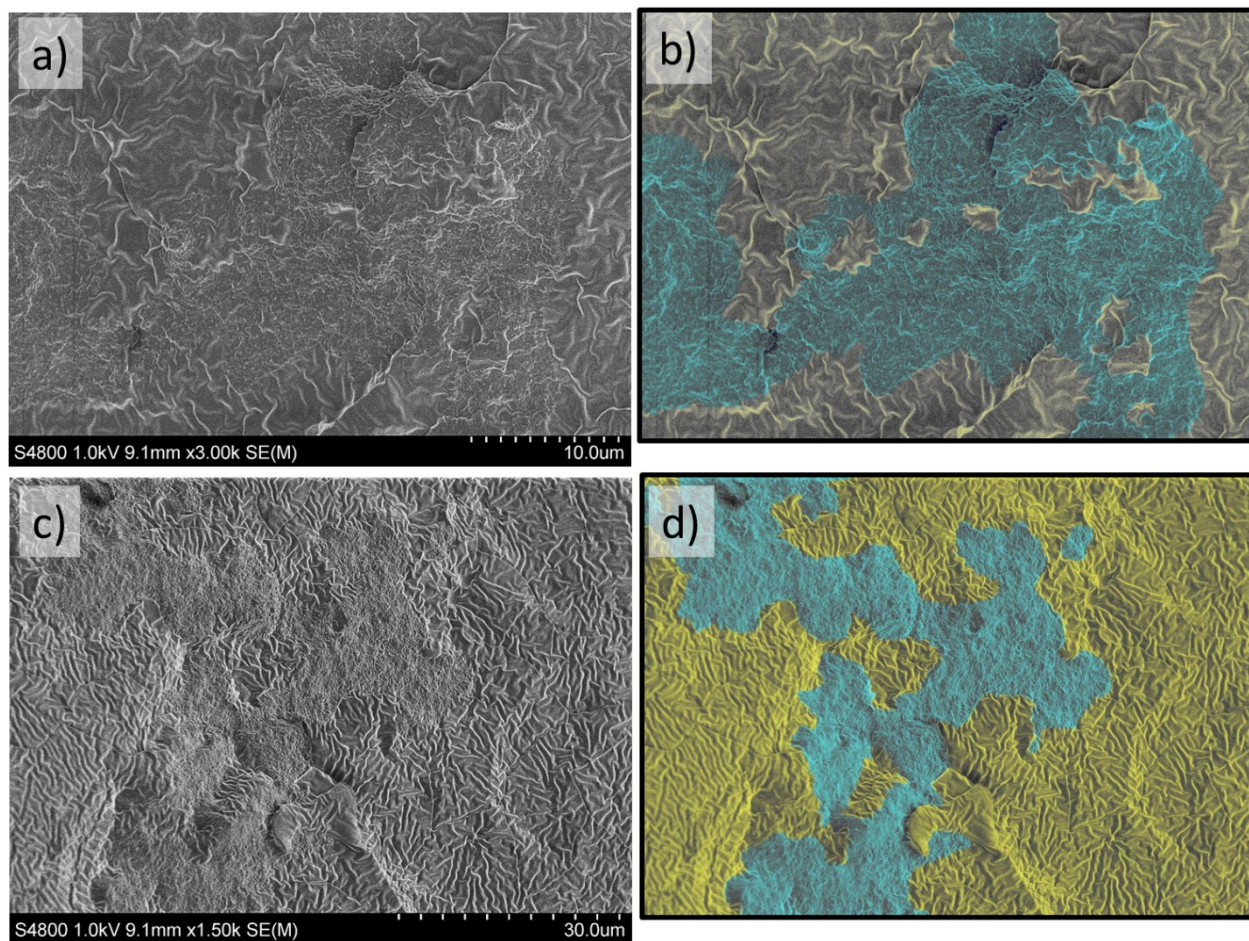


Fig.S11 a),c) Original and b),d) digitally colorized SEM image of cross-section of continuous superstructure (blue) of grafted NPs in 1.5 ZnO-g-PBMA60k. The color is used to guide the eye in order to simplify detection of NPs and superstructures.

Electrical breakdown strength

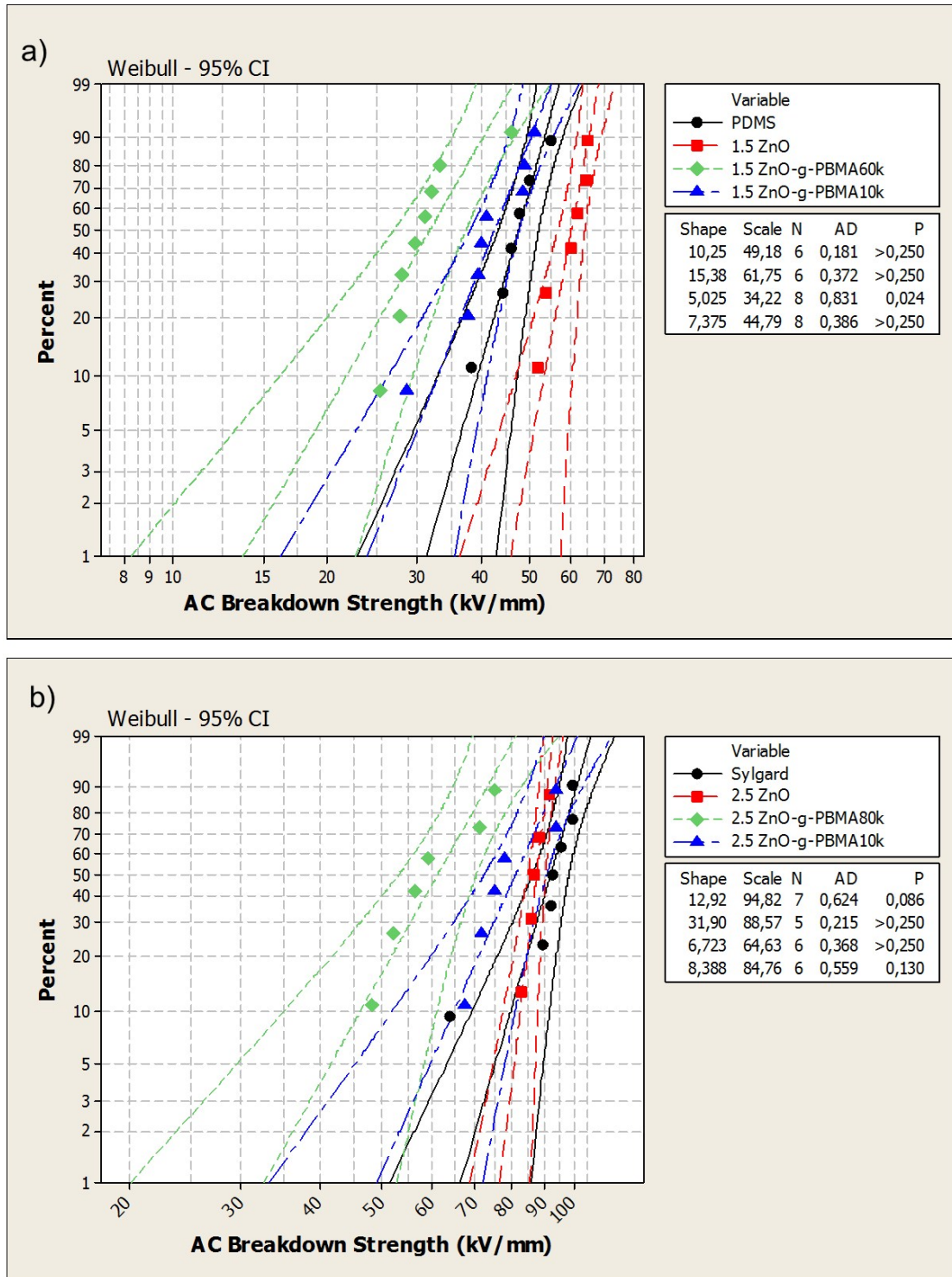


Fig.S12 Electrical breakdown strength data of a) neat PDMS, 1.5 ZnO, 1.5 ZnO-g-PBMA60k, 1.5 ZnO-g-PBMA10k (sample thickness ~ 0.6 mm), and b) neat Sylgard, 2.5 ZnO, 2.5 ZnO-g-PBMA80k, 2.5 ZnO-g-PBMA10k (sample thickness ~ 0.3 mm).

Resistivity measurements and activation energy

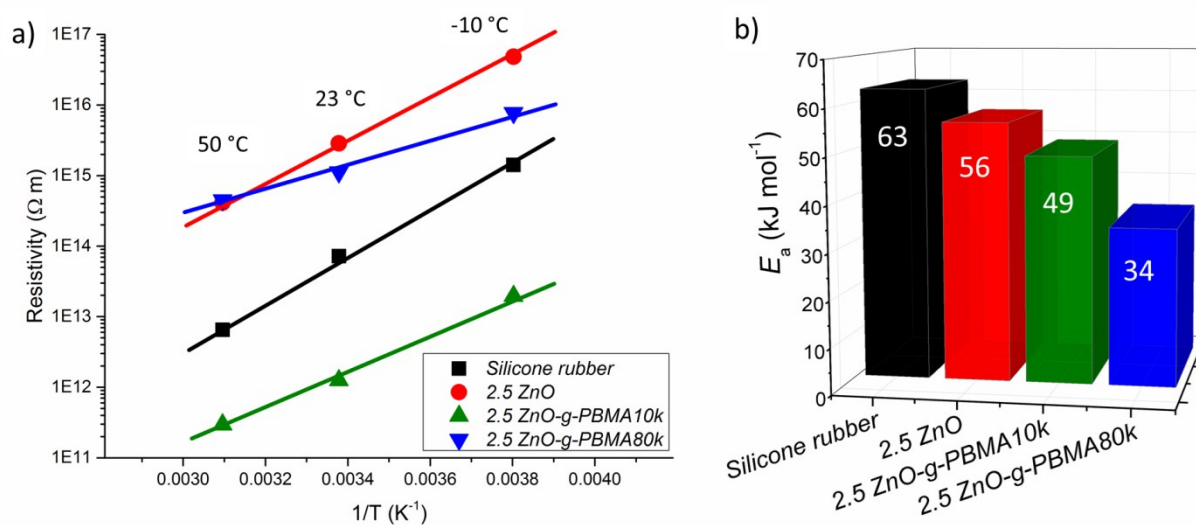


Fig.S13 The temperature dependence of the resistivity at $-10^\circ C$, $23^\circ C$ and $50^\circ C$ (a) and the activation energy (b) of Silicone rubber, 2.5 ZnO, 2.5 ZnO g PBMA10k and 2.5 ZnO g PBMA80k.

References ESI

1. C. M. Hansen, *HANSEN SOLUBILITY PARAMETERS, A User's Handbook*, CRC Press, 2nd edn., 2007.
2. Y. Wang, C. Zhang, S. Bi and G. Luo, *Powder Technology*, 2010, **202**, 130-136.
3. N. M. S. W. R. Saleh, W. A. Twej and M. Alwan, *Advances in Materials Physics and Chemistry*, 2012, **2**, 11-16.